Journal: Dalton Transaction

Manuscript ID: DT-ART-01-2023-000118

Electronic Supporting information

New Bis[cis-{MoO_2}] complexes with dihydrazone ligands: Synthesis, characterization, theoretical investigation and their peroxidase mimicking activity

Lata Rana [a,*], Dheeraj [a] and Geeta Hundal [b]

* Corresponding author: L. Rana

E-mail: latarana@chem.svnit.ac.in

[a]*Department of Chemistry, S. V. National Institute of Technology Surat, icchanath, Surat 395007*

[b] *Department of Chemistry, UGC Sponsored- Centre for Advanced Studies-II, Guru Nanak Dev University, Amritsar 143005, Punjab, India*

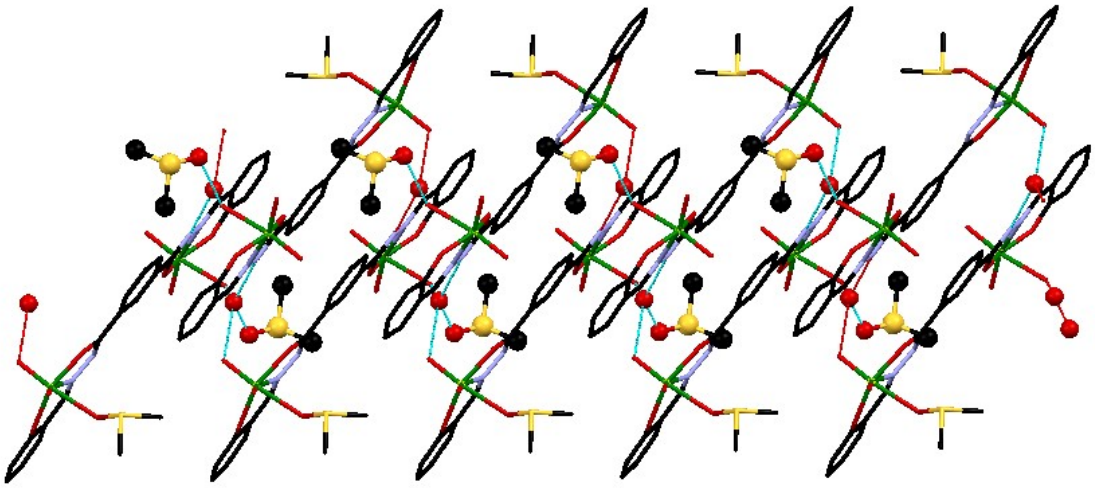

Fig. S1 In complex **1a**, various H-bonding interactions forming parallel stacking of the centrosymmetric dimeric units in the ac plane. Solvent DMSO and water molecules have been shown as balls.

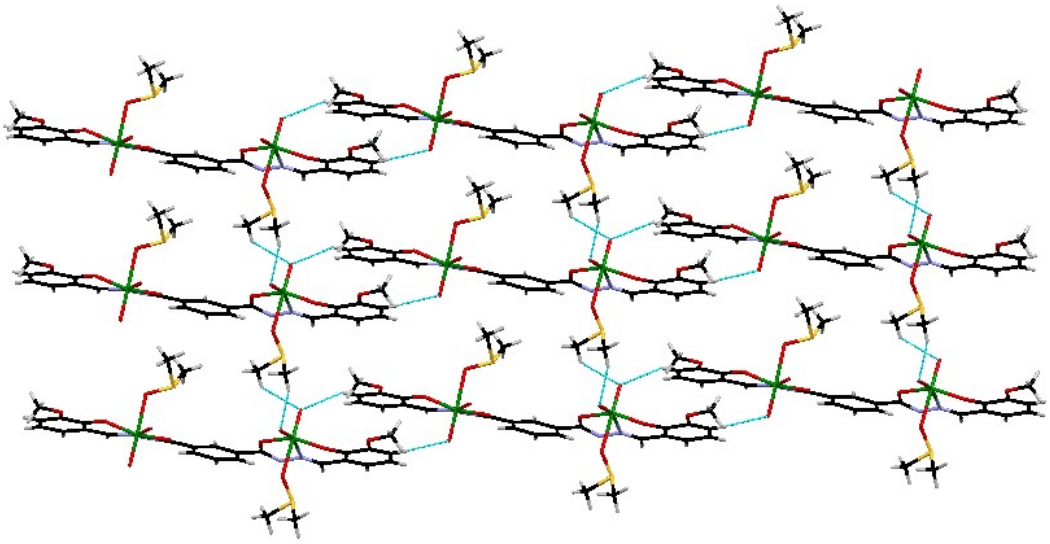

Fig. S2 In complex **2a,** various weak C-H···O H-bonding interactions forming a 2D network in the *bc* plane.

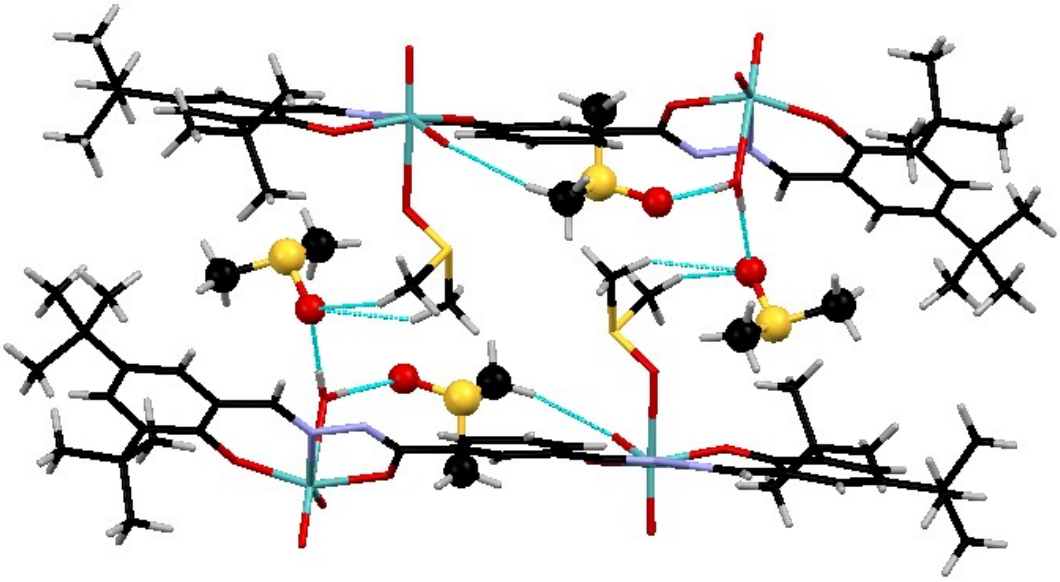

Fig. S3 In complex **3a,** various H-bonding interactions forming a centrosymmetric dimer of the binuclear units. Lattice DMSO molecules have been shown as balls.

Table S1 X-ray(experimental) and calculated (DFT/B3LYP method) selected bond lengths of complexes **1a**–**3a**

Bond length	**1a**		**2a**		**3a**	
[Å]	**Obs.**	**Calc.**	**Obs.**	**Calc.**	**Obs.**	**Calc.**
N(2)-Mo(1)	2.221(4)	2.92	2.254(7)	2.923	2.225(3)	1.970
N(3)-N(4)	1.393(5)	1.393	1.401(9)	1.398	1.400(4)	1.398
N(4)-Mo(2)	2.241(4)	2.923	2.239(6)	2.927	2.230(3)	1.960
O(1)-Mo(1)	2.011(3)	1.970	2.032(5)	1.967	2.005(2)	1.960
O(2)-Mo(1)	1.910(3)	1.907	1.906(5)	1.989	1.919(3)	1.956
O(4)-Mo(1)	1.701(3)	1.713	1.704(5)	1.712	1.709(3)	1.713
O(5)-Mo(1)	2.293(4)	1.976	1.705(6)	1.712	2.340(3)	1.970
O(7)-Mo(2)	1.922(3)	1.907	2.031(5)	1.975	1.925(2)	1.934

Table S2 X-ray(experimental) and calculated (DFT/B3LYP method) selected bond angles of complexes **1a**–**3a**

Bond Angle [°]	**1a**		**2a**		**3a**	
	Obs.	**Calc.**	**Obs.**	**Calc.**	**Obs.**	**Calc.**
O(3)-Mo(1)-O(4)	105.1(2)	105.4	104.1(2)	105.4	105.11(16)	105.8
O(3)-Mo(1)-O(2)	99.17(18)	97.8	99.17(18)	97.8	98.38(15)	97.9
O(4)-Mo(1)-O(2)	104.52(16)	104.6	104.52(16)	104.6	102.77(13)	97.0
O(3)-Mo(1)-O(1)	95.14(16)	94.6	95.14(16)	94.6	97.11(13)	97.8
O(4)-Mo(1)-O(1)	95.99(15)	95.4	95.99(15)	95.4	97.60(13)	97.4
O(2)-Mo(1)-O(1)	150.86(15)	155.4	150.86(15)	155.4	150.12(12)	151.6
O(3)-Mo(1)-N(2)	92.35(16)	94.4	92.35(16)	94.4	95.92(14)	95.8
O(4)-Mo(1)-N(2)	159.87(18)	155.7	159.87(18)	155.7	157.83(14)	161.4
O(2)-Mo(1)-N(2)	82.07(14)	80.5	82.07(14)	80.5	80.62(11)	80.9
O(1)-Mo(1)-N(2)	72.06(13)	77.5	82.07(14)	80.5	80.62(11)	80.9
O(3)-Mo(1)-O(5)	168.27(16)	171.3	168.27(16)	171.3	169.96(14)	169
O(4)-Mo(1)-O(5)	86.08(18)	87.5	86.08(18)	87.5	84.46(13)	88.9
O(2)-Mo(1)-O(5)	81.11(16)	80.7	81.11(16)	80.7	82.13(12)	79.8
O(1)-Mo(1)-O(5)	79.86(14)	74.5	79.86(14)	74.5	78.31(11)	79.6
N(2)-Mo(1)-O(5)	76.05(15)	77.6	76.05(15)	77.6	74.22(11)	74.7
O(8)-Mo(2)-O(7)	102.71(17)	97.4	102.71(17)	97.4	98.69(14)	97.9
O(8)-Mo(2)-O(6)	97.42(16)	97.6	97.42(16)	97.6	94.44(13)	95.5
O(7)-Mo(2)-O(6)	150.08(15)	151.5	150.08(15)	151.5	150.70(11)	151.5
O(8)-Mo(2)-N(4)	159.34(19)	155.3	159.34(19)	155.3	94.03(13)	95.4
O(7)-Mo(2)-N(4)	82.72(14)	80.3	82.72(14)	80.3	80.93(11)	80.5
O(6)-Mo(2)-N(4)	71.07(13)	74.3	71.07(13)	74.3	72.09(10)	74.8

Table S3 The Mulliken atomic charges of all the ligands calculated by B3LYP/6-31G(d,p) method.

Atoms	I	II	III	Atoms	I	II	III
C1	-3.03247	-8.11089	-6.3714	C25	3.49672	6.7115	4.44141
C2	-1.91228	-8.45356	-5.61044	C26	-0.82998	6.38285	4.95835
C3	-1.43186	-7.4495	-4.0752	C27	-3.3648	9.03572	4.27413
C4	-2.1174	-6.21641	-3.48545	O28	-1.36769	8.50594	4.85133
C5	-3.39681	-5.82534	-4.35043	N29	-1.77565	-6.33929	4.1384
C6	-3.83468	-6.71287	-5.70112	N30	-4.73398	-7.13601	4.71804
O7	-4.15593	-4.51485	-3.72826	C31	-3.93207	-8.80276	5.94036
C8	-0.15822	-5.20561	-1.95042	C32	0.97107	-9.42299	6.74995
N9	-5.22619	-4.10994	-1.3895	C33	1.97209	-7.7272	6.24027
N10	0.18514	-3.94917	-2.17974	C34	3.81344	-4.53456	6.99234
C11	-3.57762	-1.58853	0.09233	C35	5.89537	-5.41274	8.13878
C12	0.64077	-3.07569	-1.4453	C36	6.75045	-4.85702	8.44783
O13	1.73022	-3.54289	-2.07383	C37	5.54768	-1.70594	8.16208
C14	2.33644	-1.08665	-6.2813	O38	-1.95933	0.77169	9.60065
C15	3.57018	0.37489	-7.66006	C39	-1.45598	2.16581	3.90907
C16	4.17937	1.15905	-6.45667	C40	-3.67083	-1.04127	3.03144
C17	5.41853	0.59913	-5.39821	C41	-5.74358	2.905	3.80954
C18	5.89425	-0.67303	-6.56548	C42	-5.4599	3.4453	5.28587
C19	5.1884	1.47841	-7.37827	C43	3.94531	5.12373	-7.43796
C20	4.11507	1.09343	-5.329	C44	-0.17132	7.55992	-3.47431
C21	-3.91457	2.76523	-7.62125	C45	3.49672	6.7115	4.44141
C22	-2.96451	3.85557	0.77154	C46	-0.82998	6.38285	4.95835
C23	-3.20195	4.17199	2.3092	H47	-3.3648	9.03572	4.27413
C24	-2.12595	5.60621	2.983	H48	-1.36769	8.50594	4.85133

Table S4 The Mulliken atomic charges of all complexes calculated by B3LYP/LANL2DZ method.

Atoms	Complex 1	Complex 2	Complex 3	ATOMS	Complex 1	Complex 2	Complex 3
Mo1	-0.51854	-0.51854	-0.60965	C29	0.72113	1.92618	0.84412
O2	-1.26828	-1.26828	-1.45616	N30	1.92618	0.80657	1.14597
O3	-1.91807	-1.91807	-1.93166	Mo31	0.80657	1.08111	3.3404
O4	-1.32533	-1.32533	-1.47486	O32	1.08111	3.31059	2.97101
O5	0.20391	0.20391	0.15925	O33	3.31059	2.7619	1.64771
N6	0.54099	0.54099	0.58505	O34	2.7619	1.61886	3.32899
O7	1.72789	1.72789	1.4437	O35	1.61886	3.22925	5.18893
H8	2.54817	2.54817	2.30854	N36	3.22925	5.11425	3.78551
H9	1.75729	1.75729	1.41344	O37	5.11425	3.83572	3.34189
C10	-1.04133	-1.04133	-1.05117	H38	3.83572	3.56689	3.60769
C11	-0.56376	-0.56376	-0.43879	H39	3.56689	3.92824	2.46023
C12	0.26698	0.26698	0.51529	C40	3.92824	2.70242	2.95342
C13	0.65062	0.65062	0.88351	N41	2.70242	2.88857	3.26368
C14	0.20376	0.20376	0.30747	C42	2.88857	3.27302	5.3319
C15	-0.69695	-0.69695	-0.71638	C43	3.27302	5.45114	5.83486
H16	-1.68297	-0.83888	-0.70394	C44	5.45114	6.06674	5.61769
H17	-0.83888	0.61254	1.61772	C45	6.06674	5.61726	6.58624
C18	0.61254	1.29456	0.85834	H46	5.61726	6.80026	5.64079
C19	1.29456	0.75322	1.87723	C47	6.80026	5.97439	6.36395
C20	0.75322	1.79286	1.20849	C48	5.97439	6.32944	6.84565
C21	1.79286	1.11939	0.87506	H49	6.32944	6.91443	7.41304
C22	1.11939	0.74253	1.21684	C50	6.91443	7.26841	4.4922
C23	0.74253	1.02551	1.88967	H51	7.26841	7.4512	4.49606

C24	1.02551	1.708	2.21802	H52	6.431	4.62326	1.51556
H25	1.708	2.10454	2.1285	C53	7.4512	4.69498	-2.83789
H26	2.10454	2.07516	0.36043	H54	4.62326	1.35256	-2.12915
H27	2.07516	0.23848	0.96423	H55	4.69498	6.46504	-3.57366
H28	0.23848	0.72113	2.15198	H56	1.35256	-1.89883	-3.31556

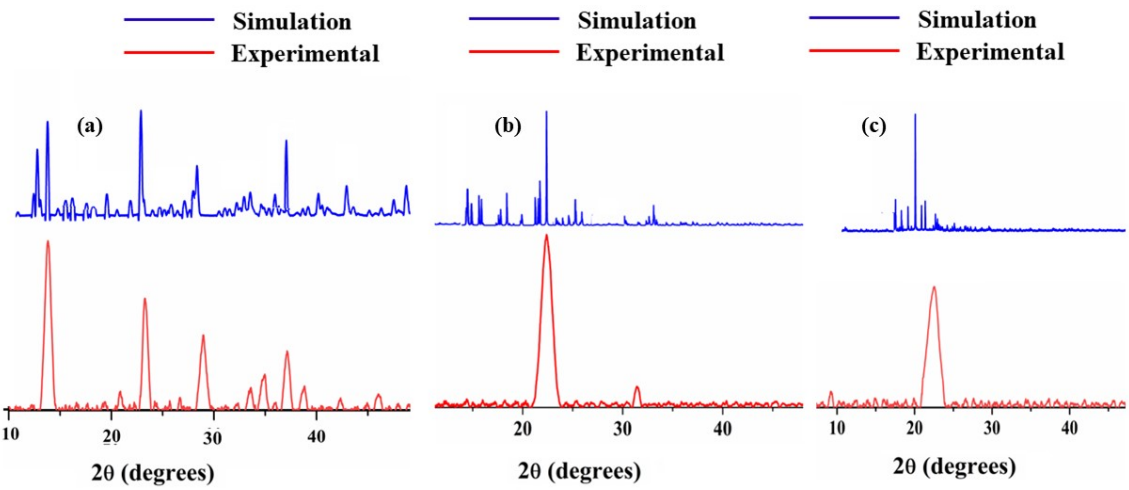

Fig S4 Powder XRD patterns for **(a)** complex **1, (b)** complex **2** and **(c)** complex **3.**

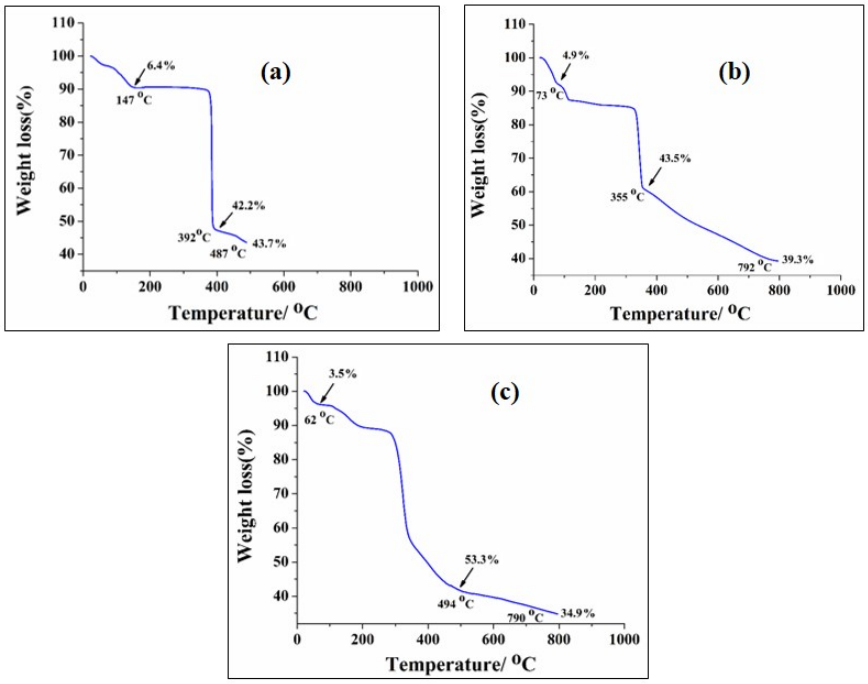

Fig. S5 TGA profiles for **(a)** complex $[\{Mo^{VI}O_2\}_2(L^1)(H_2O)_2]$ **1, (b)** complex $[\{Mo^{VI}O_2\}_2(L^2)(H_2O)_2]$ **2**, and (c) complex $[\{Mo^{VI}O_2\}_2(L^3)(H_2O)_2]$ **3.**

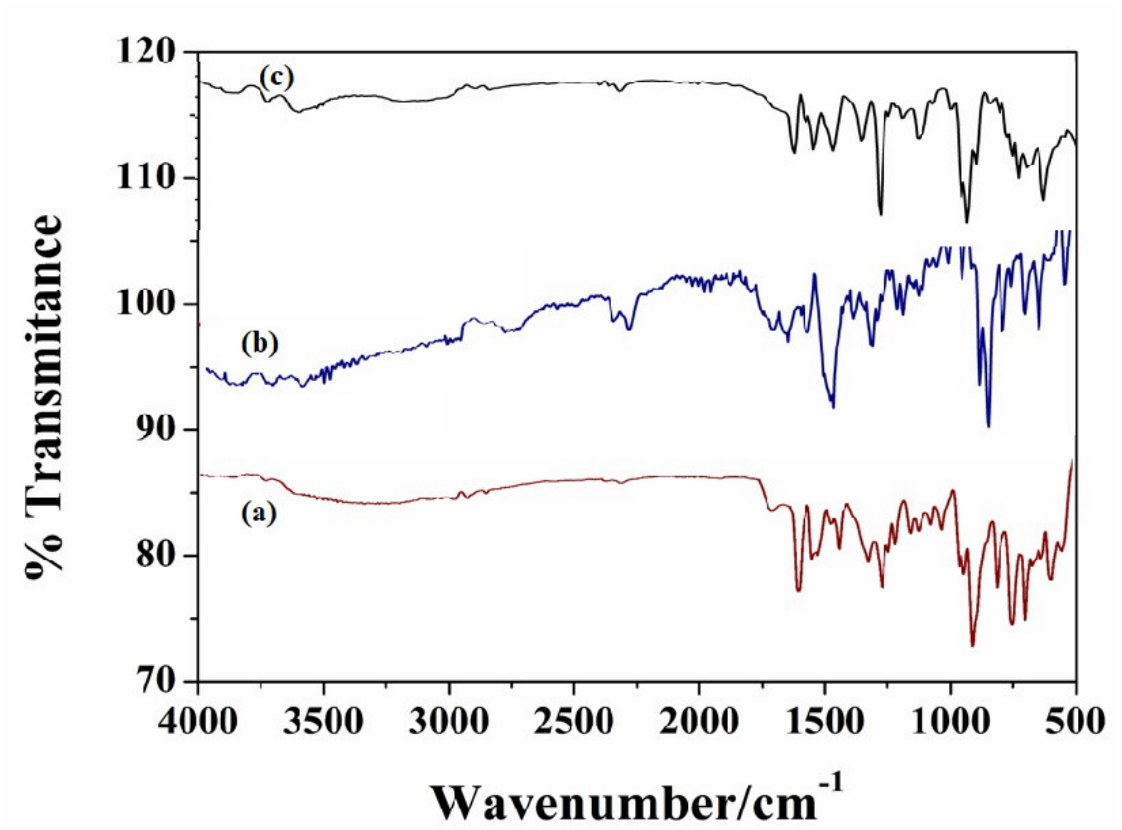

Fig. S6 IR spectra of all binuclear molybdenum complexes for **(a)** complex **1**, **(b)** complex **2**, **(c)** complex **3** recorded experimentally.

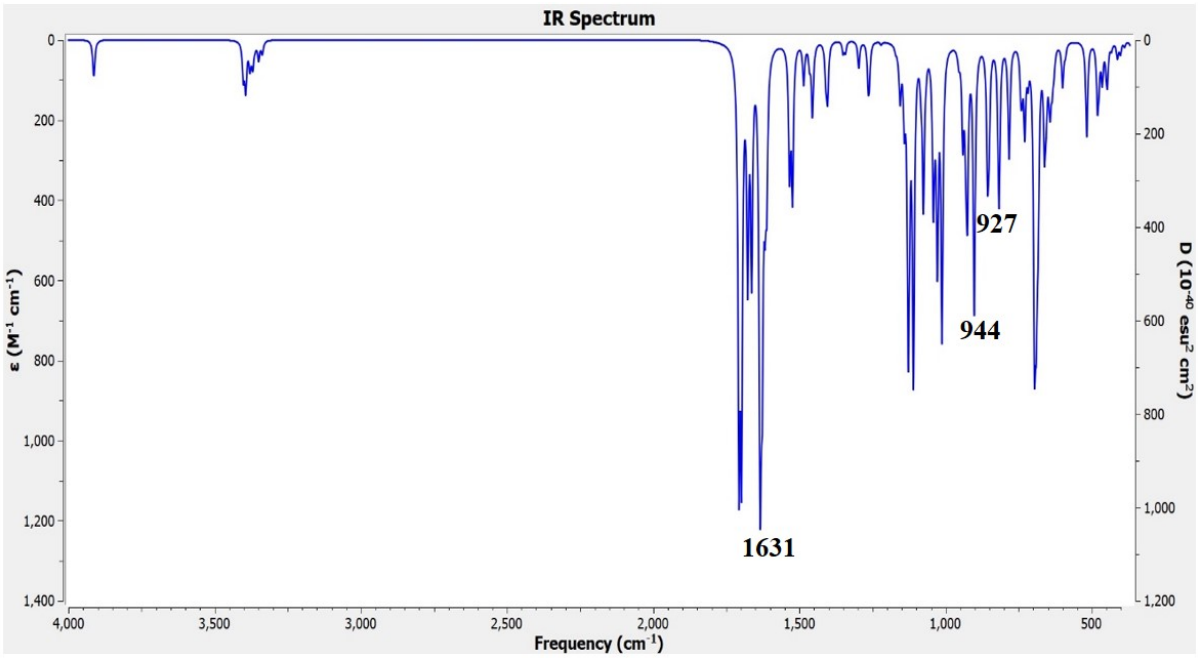

Fig. S7 Theoretical IR spectra of complex **1.**

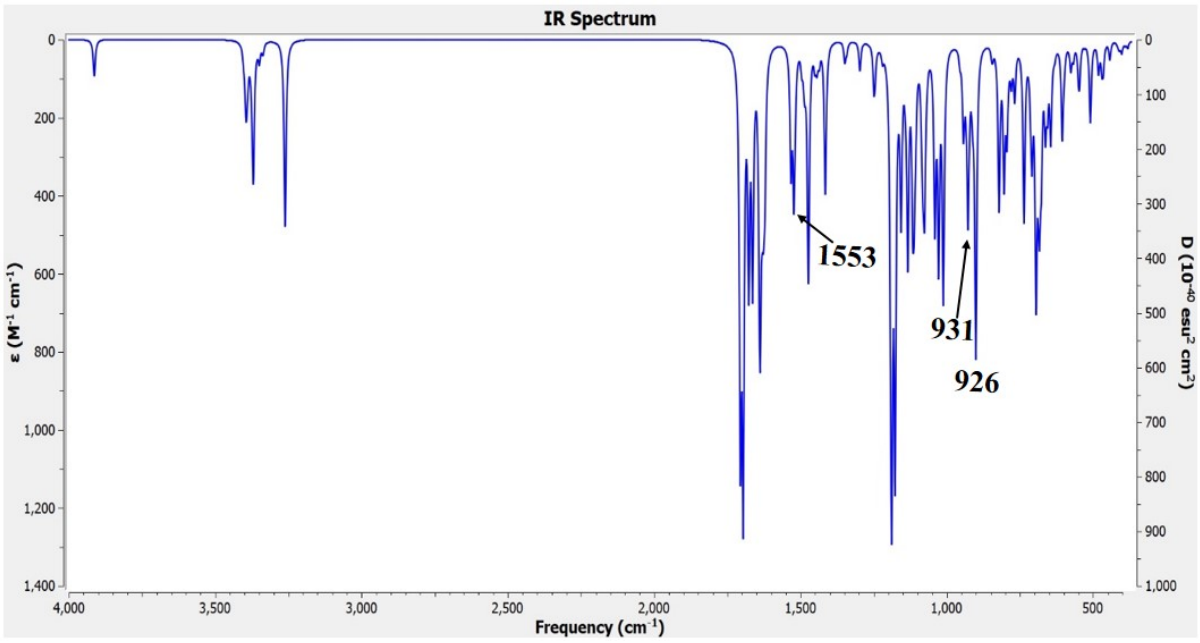

Fig. S8 Theoretical IR spectra of complex **2.**

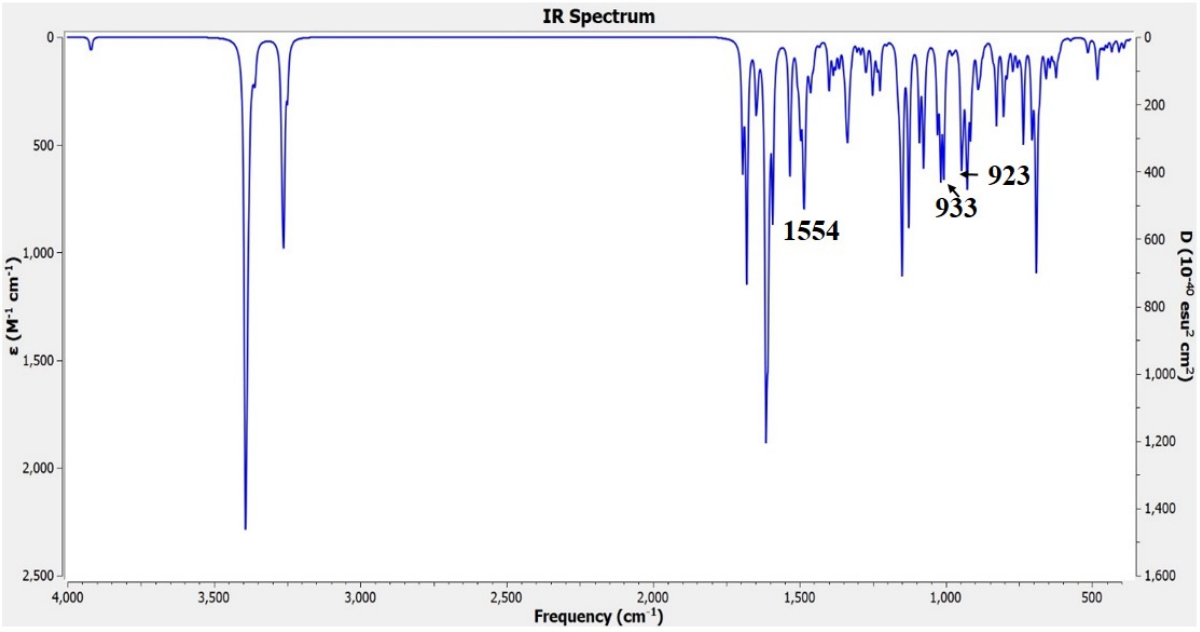

Fig. S9 Theoretical IR spectra of complex **3.**

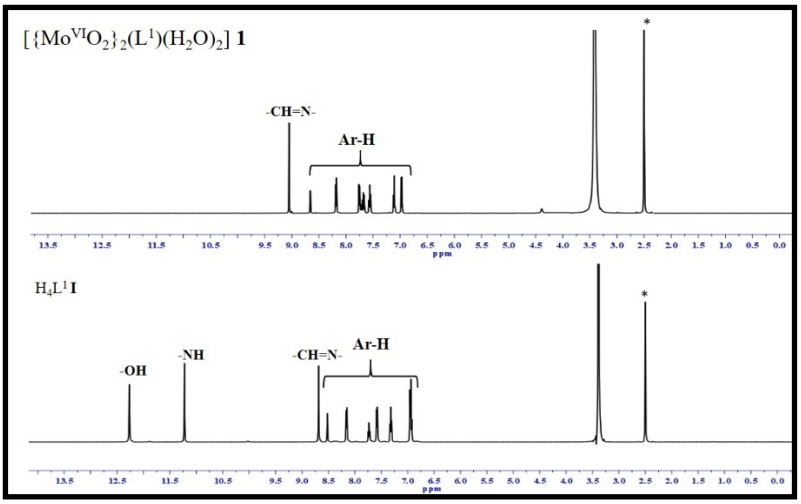

Fig. S10 ^{1}H-NMR spectra of ligand **I** and complex **1** were recorded in DMSO-D_6. * represents the DMSO solvent peak.

Table S5 The calculated and theoretical chemical shifts(δ) values in ppm of the ligands and their complexes as determined by ^{1}H NMR in DMSO-d_6.

Compound	values	Phenolic (–OH)	–NH	–OCH_3	tert-butyl	–CH=N–	Aromatic protons
I	**Exp.**	12.27 (br, 2H)	11.22 (s, 2H)	–	–	8.68 (s, 2H)	8.52(s, 1H), 8.15–8.16(d, 2H), 7.71–7.74(t, 1H), 7.57–7.59(d, 2H), 7.30–7.33(t, 2H), 6.92–6.96(m, 4H)
	Calc.	10.00 (br, 2H)	9.30 (s, 2H)			8.70 (s, 2H)	8.70(s, 1H), 8.10(d, 2H), 7.90(t, 1H), 7.50(d, 2H), 7.20(t, 2H), 6.90(m, 4H
1	**Exp.**	–	–	–	–	9.05 (s, 2H)	8.66(s, 1H), 8.17–8.19(d, 2H), 7.74–7.76(t, 1H), 7.68–7.70(d, 2H), 7.54–7.58(t, 2H), 7.09–7.12(t, 2H), 6.97–6.98(d, 2H)
	Calc.	–	–	–	–	8.50 (s, 2H)	8.56(s, 1H), 8.40(d, 2H 7.70(t, 1H), 7.40(d, 2H), 7.30(t, 2H), 7.20(t, 2H), 6.90(d, 2H)
II	**Exp.**	12.27(br, 2H)	10.89(s, 2H)	3.81(s, 6H)	–	8.69 (s, 2H)	8.51(s, 1H), 8.14-8.16(d, 2H), 7.70-7.74(t, 1H), 7.17-7.19(d, 2H), 7.03-7.05(d, 2H)6.85-6.89(t, 2H)
	Calc.	10.4 (br, 2H)	10.10 (s, 2H)	3.70 (s, 6H)		8.80 (s, 2H)	8.80(s, 1H), 8.10(d, 2H),7.70(t, 1H), 7.20(d, 2H), 7.10(d, 2H),6.80(t, 2H)
2	**Exp.**	–	–	3.81(s, 6H)	–	9.02 (s, 2H)	8.65 (s, 1H), 8.17–8.18(d, 2H), 7.66–7.69(t, 1H), 7.31–7.33(d, 2H), 7.25–7.27(d, 2H), 7.03–7.06(t, 2H)
	Calc.	–	–	2.80 (s, 6H)		8.50 (s, 2H)	8.40 (s, 1H), 8.50(d, 2H), 7.70(t, 1H), 7.70(d, 2H), 7.50(d, 2H), 7.30(t, 2H)

III	**Exp.**	12.39 (br, 2H)	12.23(s, 2H)	–	1.42(s, 18 H), 1.29(s, 18 H)	8.61 (s, 2H)	8.50(s, 1H), 8.16–8.17(d, 2H), 7.75–7.78(t, 1H), 7.33(s, 2H), 7.24(s, 2H)
	Calc.	10.25 (br, 2H)	10.15 (s, 2H)	–	1.08 (s, 18 H), 0.96 (s, 18 H)	8.45 (s, 2H)	8.56(s, 1H), 8.10–8.20(d, 2H), 7.66–7.69(t, 1H), 7.22(s, 2H), 7.19(s, 2H)
3	**Exp.**	–	–	–	1.37(s, 18H) 1.31 (s, 18H)	9.04 (s, 2H)	8.64(s, 1H), 8.17–8.19(d, 2H), 7.66–7.69(t, 1H), 7.54(s, 2H), 7.53(s, 2H)
	Calc.	–	–	–	0.80 (s, 18H) 0.90 (s, 18H)	8.40 (s, 2H)	8.40(s, 1H), 8.30(d, 2H), 7.80(t, 1H), 7.60(s, 2H), 7.40(s, 2H)

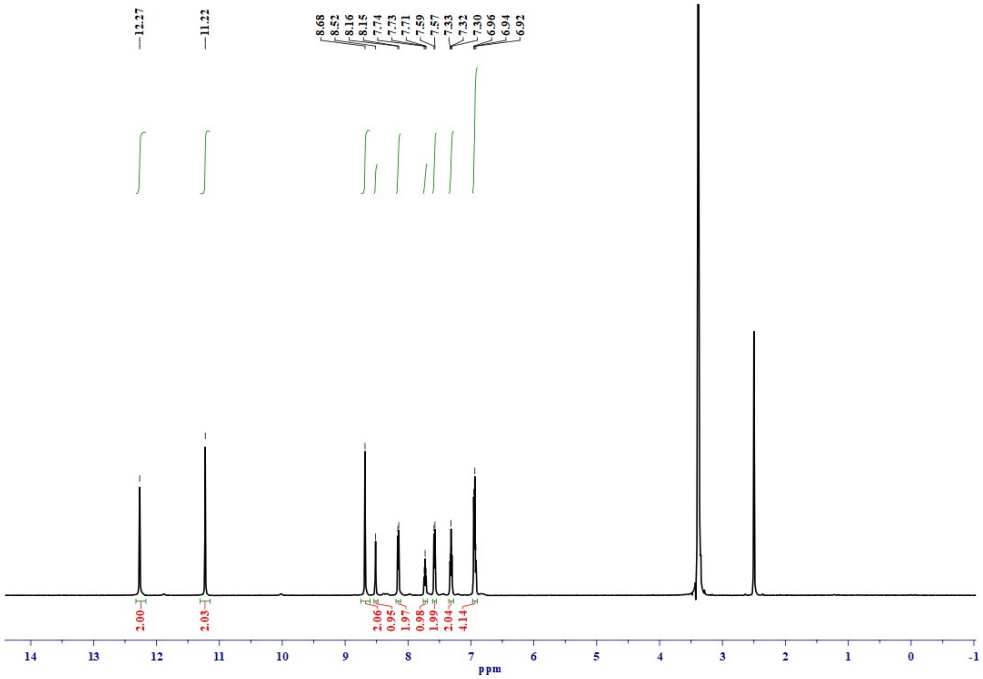

Fig. S11 ^{1}H-NMR spectra of Ligand **I**.

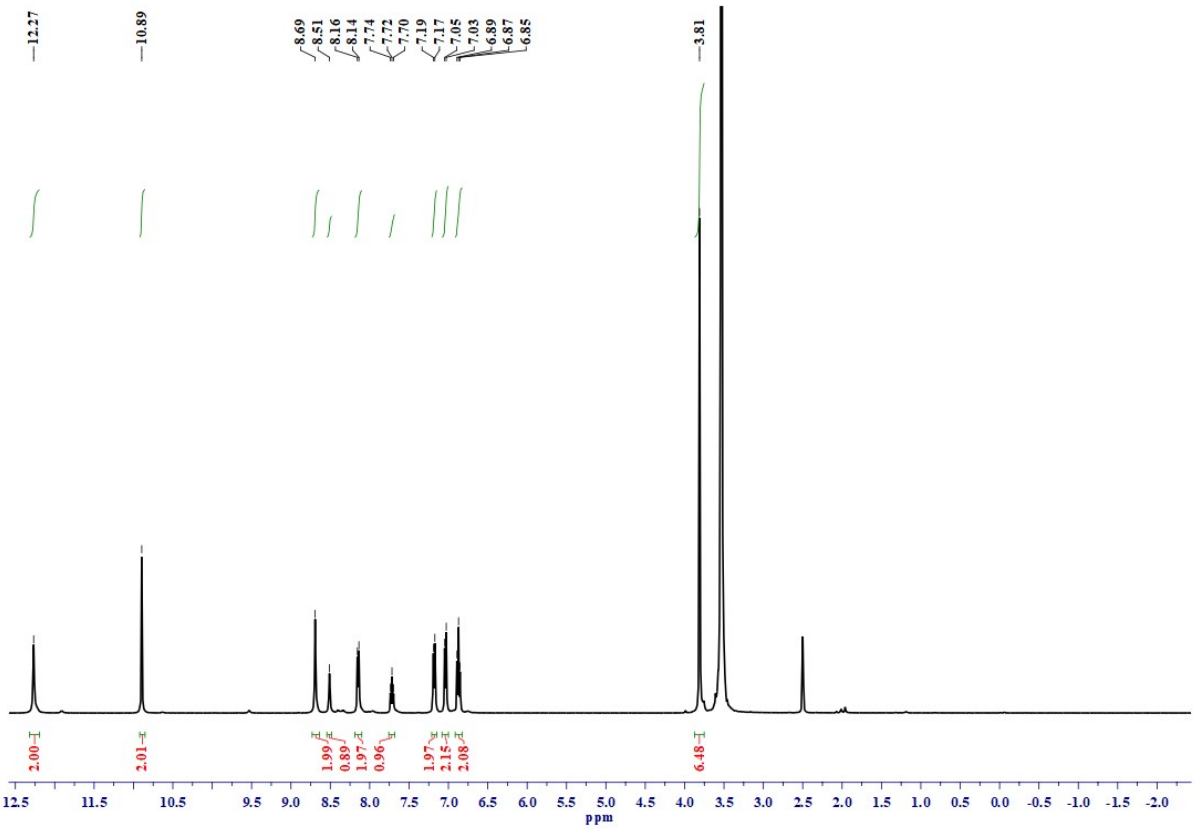

Fig. S12 ^{1}H-NMR spectra of Ligand **II**.

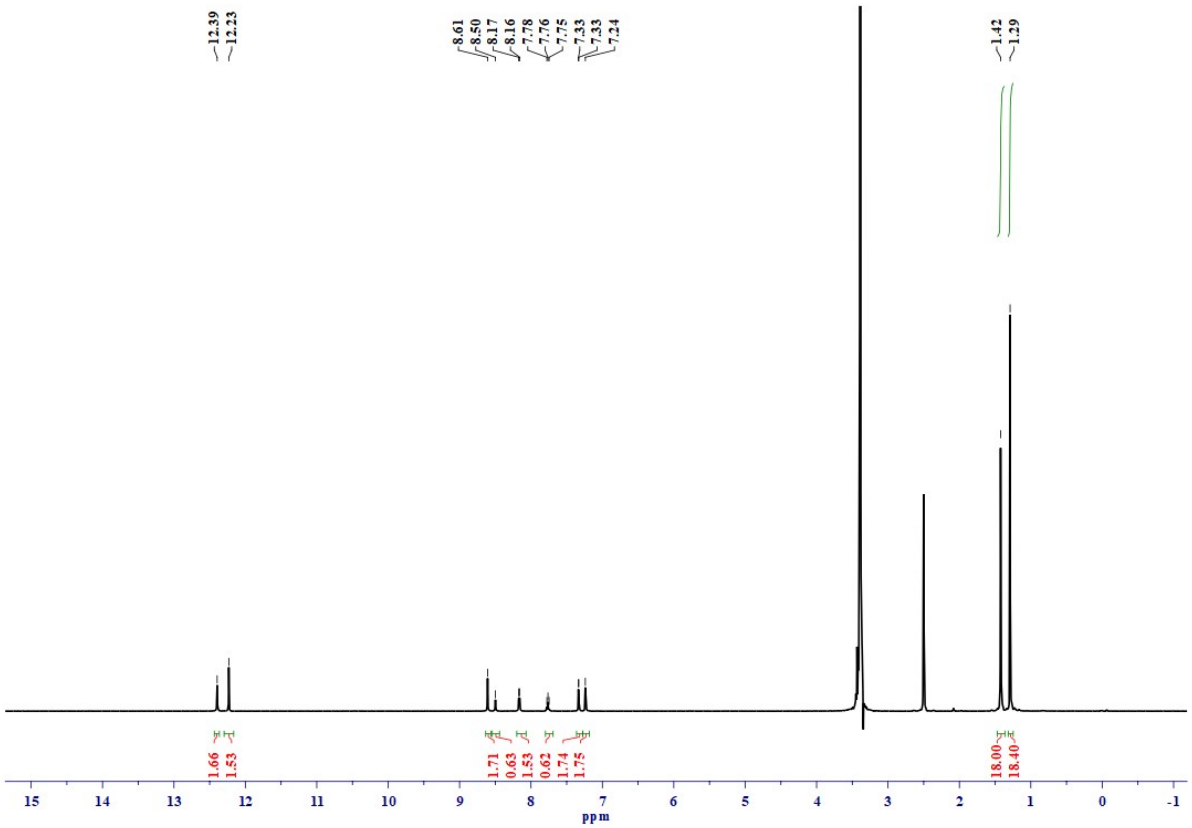

Fig. S13 [1]H-NMR spectra of Ligand **III**.

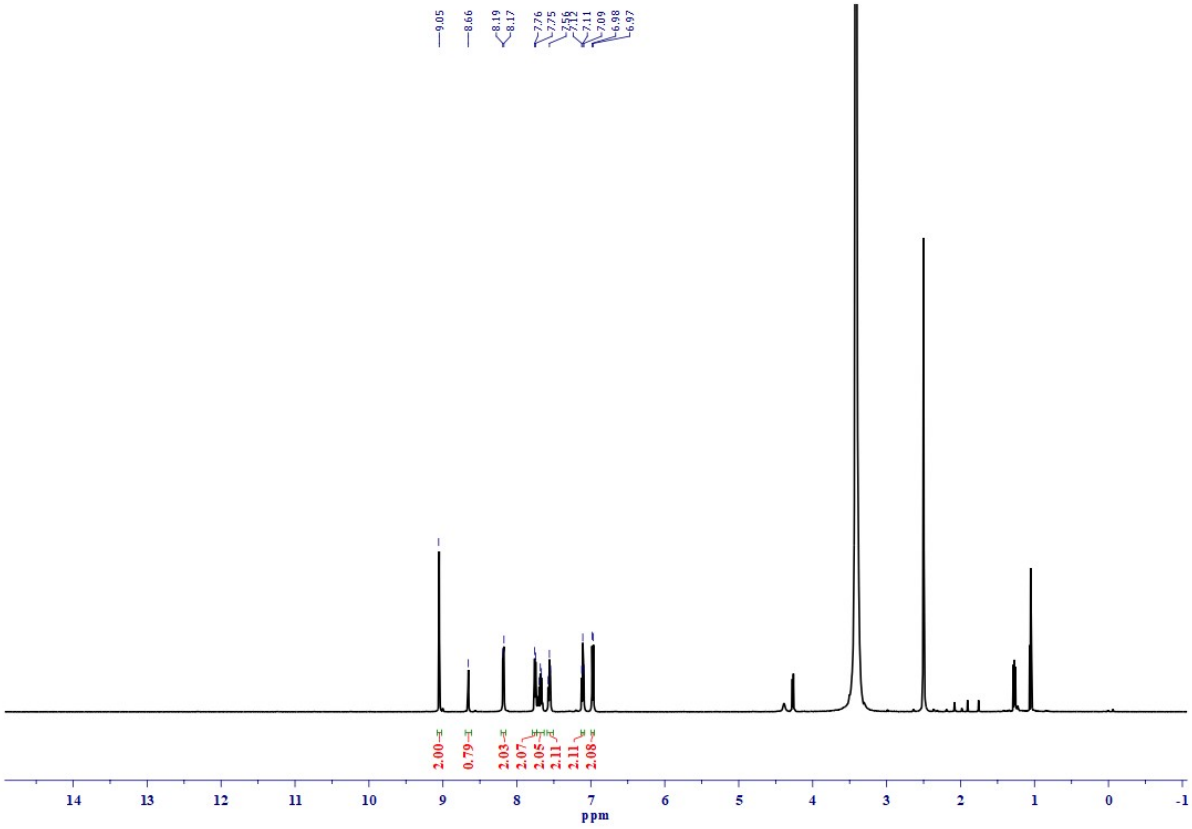

Fig. S14 [1]H-NMR spectra of complex **1**.

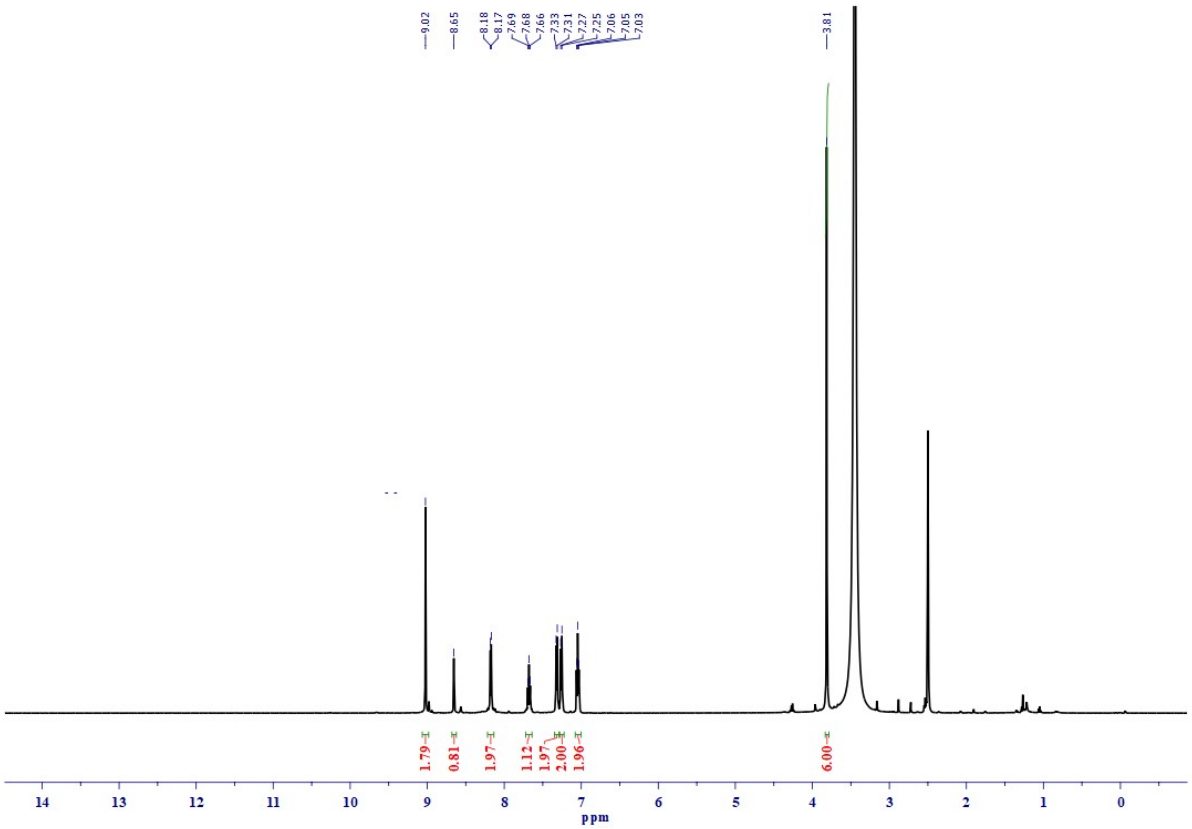

Fig. S15 [1]H-NMR spectra of Complex **2**.

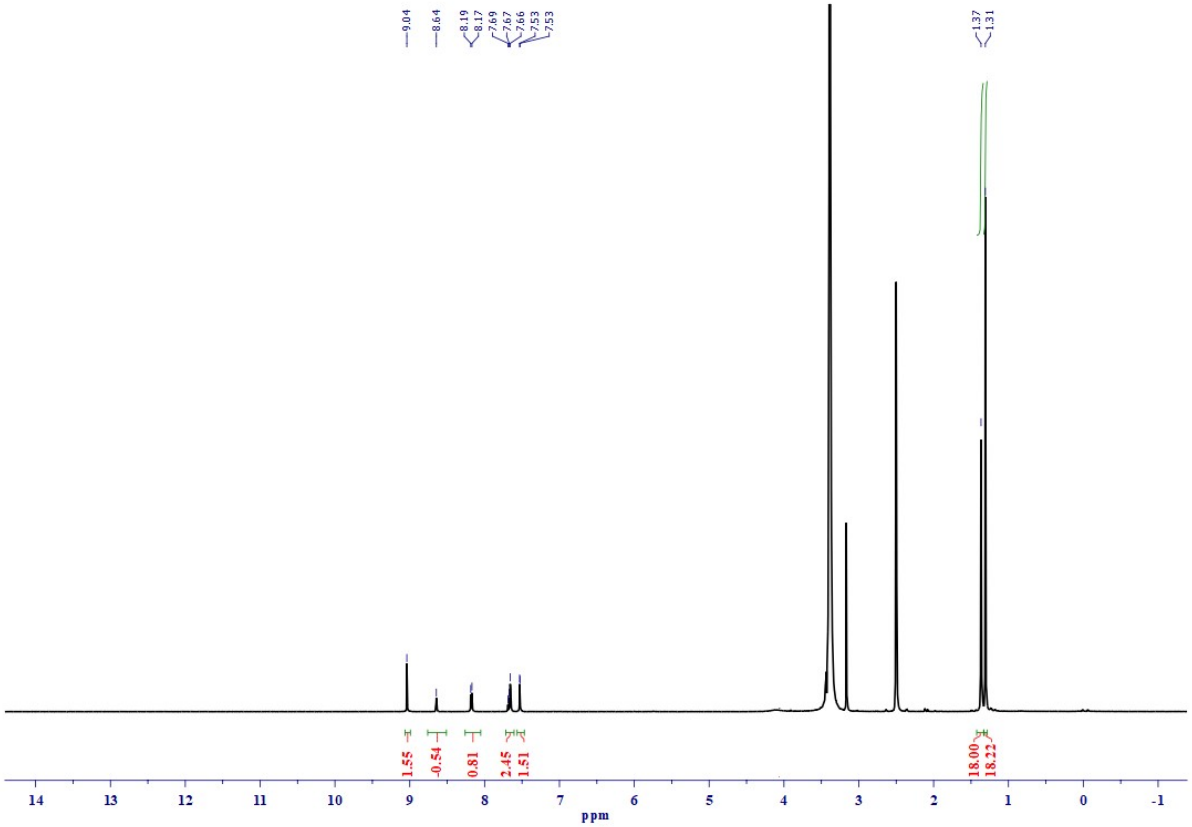

Fig. S16 [1]H-NMR spectra of Complex **3**.

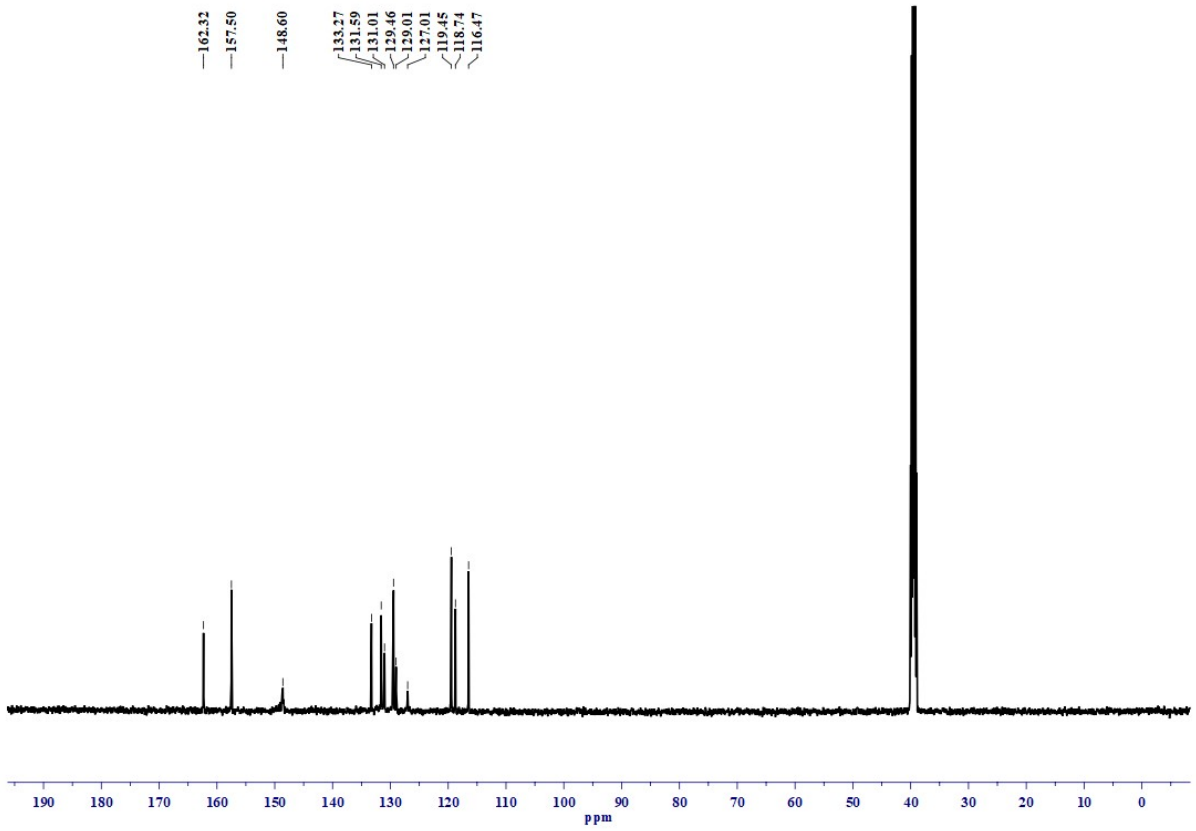

Fig. S17 ^{13}C-NMR spectra of Ligand **I**.

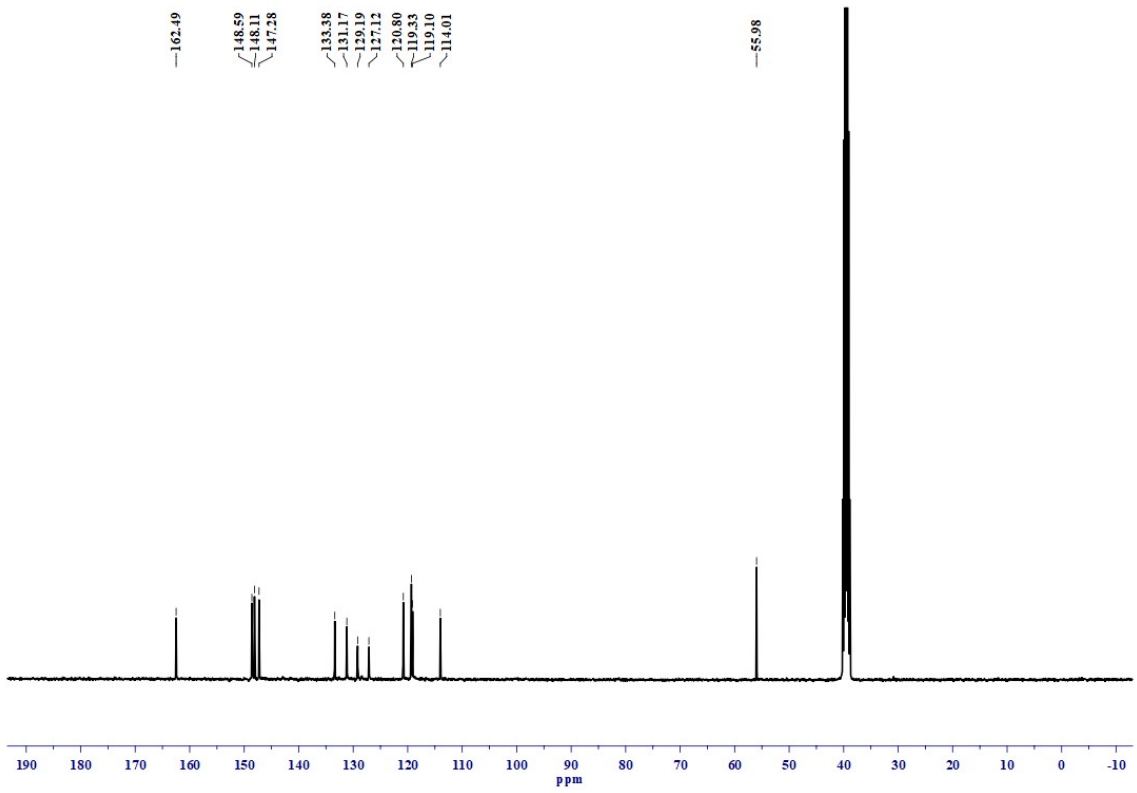

Fig. S18 ^{13}C-NMR spectra of Ligand **II**.

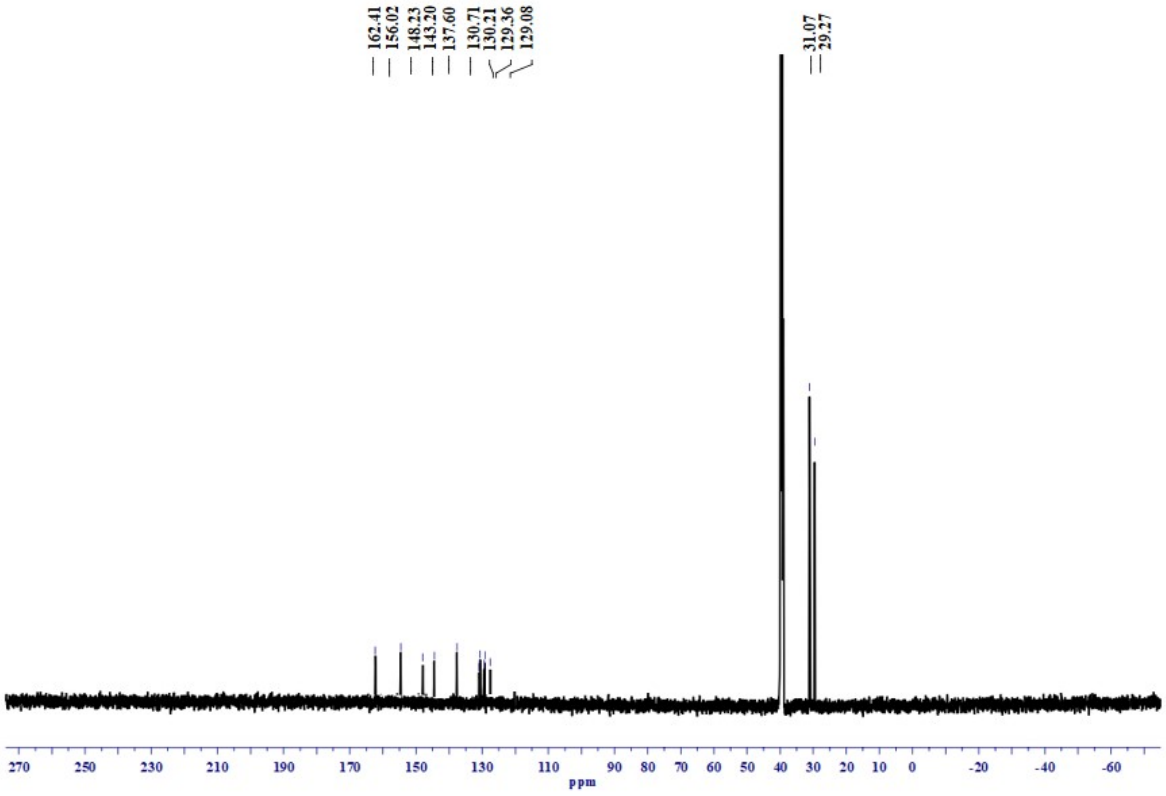

Fig. S19 ^{13}C-NMR spectra of Ligand **III**.

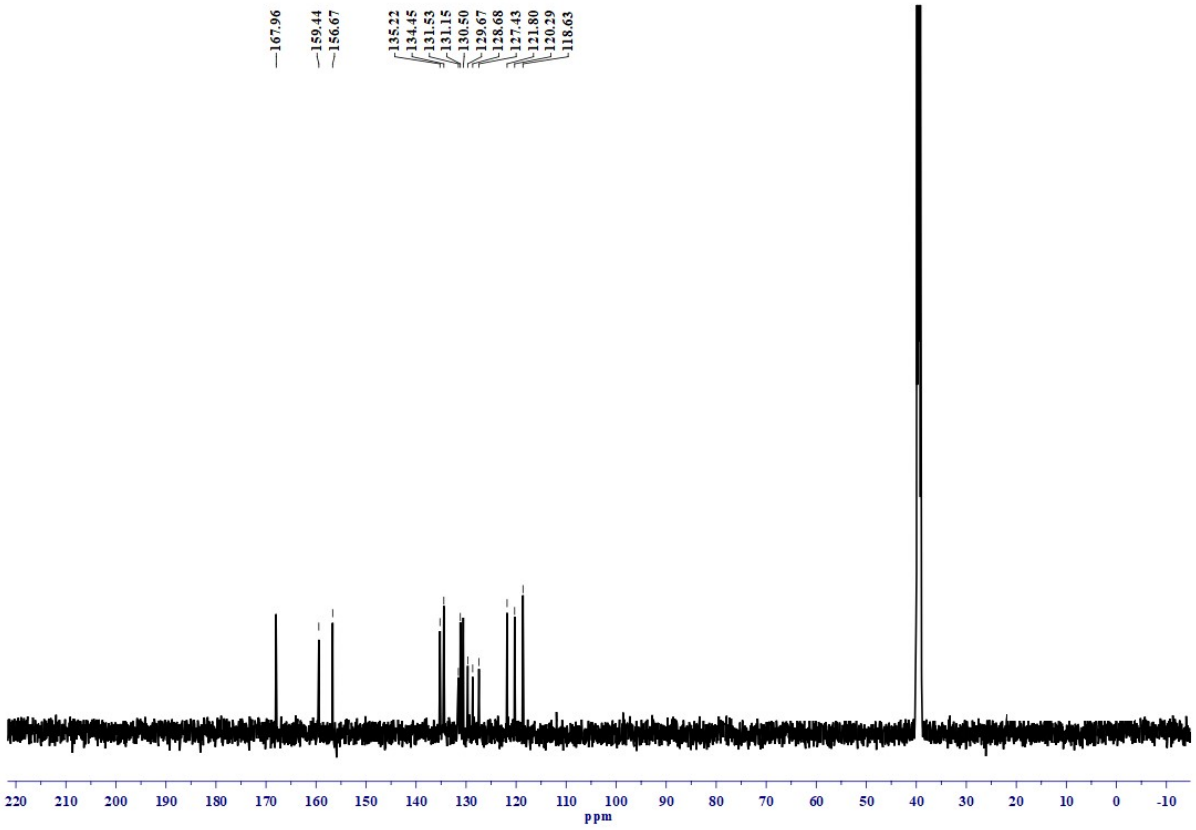

Fig. S20 ^{13}C-NMR spectra of complex **1**.

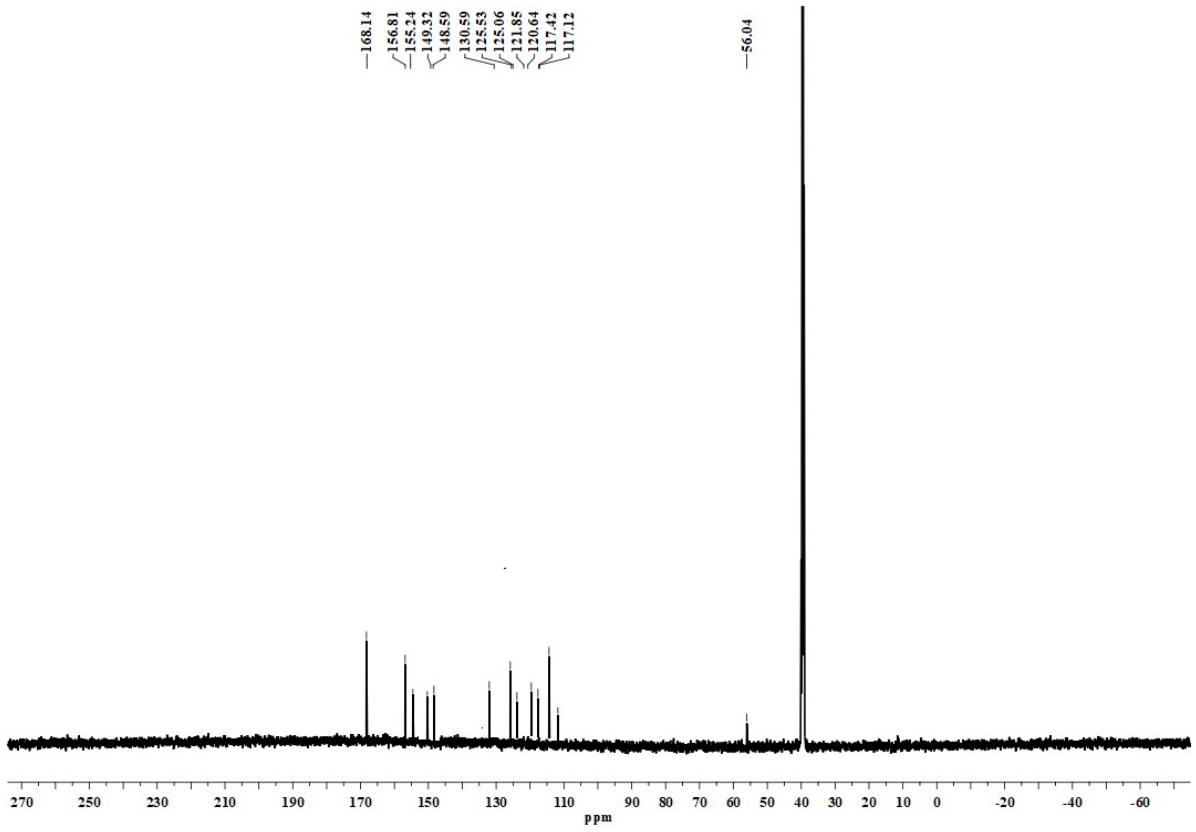

Fig. S21 ^{13}C-NMR spectra of complex **2.**

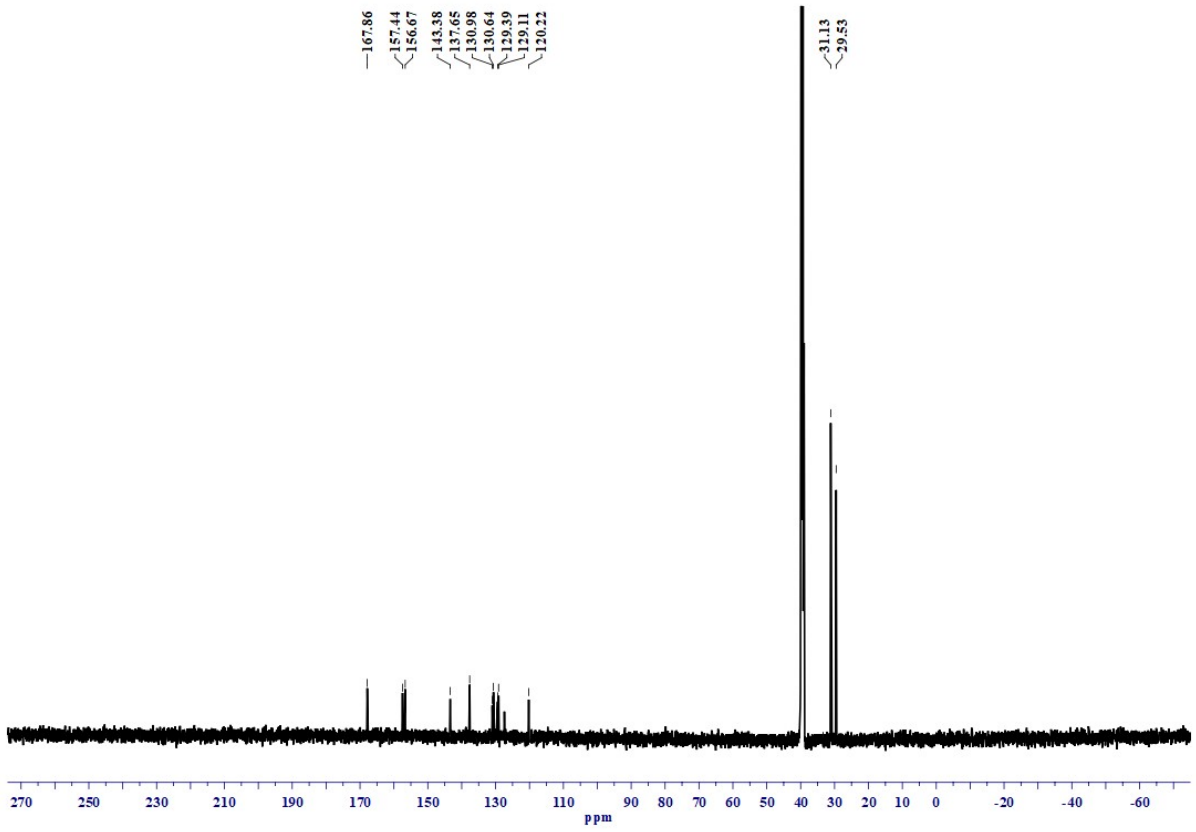

Fig. S22 ^{13}C-NMR spectra of complex **3**.

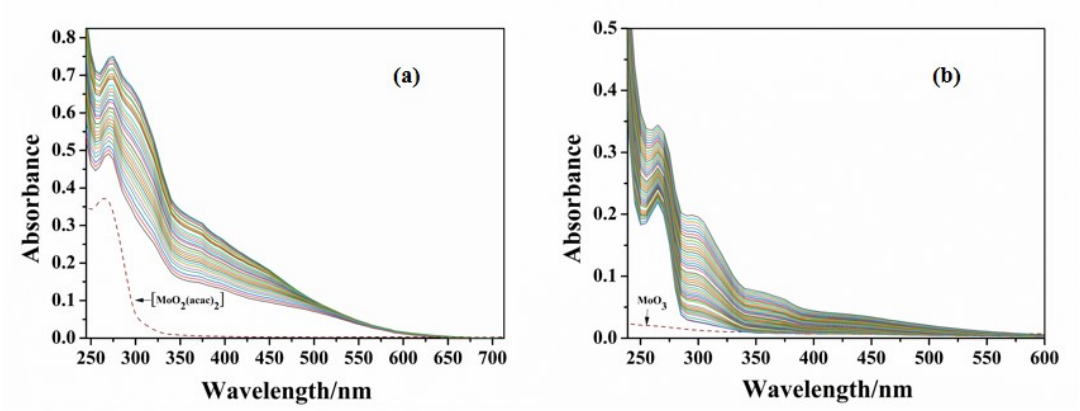

Fig. S23 (a) The optimal reaction conditions for pyrogallol peroxidase activity were pyrogallol solution (1 mL, 2.5 ×10^{-2} M), [MoO_2(acac)$_2$] (0.004 g), 30% H_2O_2 (1 mL, 2.5 × 10^{-4} M), pH 7 phosphate buffer (1 mL, 1 M), and reaction temperature (25^o C), with no visible band at λ_{max}=420 nm; (b) pyrogallol solution (1 mL, 2.5 ×10^{-2} M), MoO_3 (0.004 g), 30% H_2O_2 (1 mL, 2.5 × 10^{-4} M), pH 7 phosphate buffer (1 mL, 1 M), and reaction temperature (25^o C) were used, and no discernible band was found at λ_{max} =420 nm.

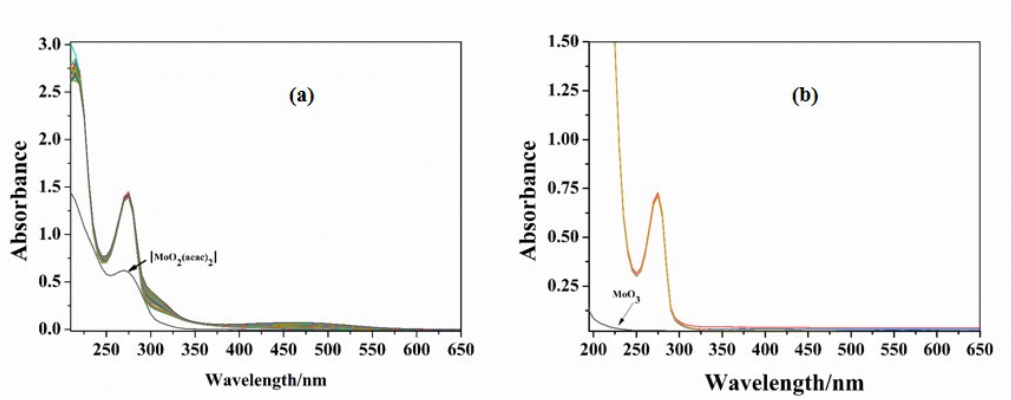

Fig. S24 (a) The optimal reaction conditions for dopamine peroxidase activity were dopamine 1 mL, 2 × 10^{-3} M) in MeOH, $[MoO_2(acac)_2]$ (2.0 × 10^{-4} M), 30% H_2O_2 (1 mL, 2× 10^{-3} M), pH 7 phosphate buffer (1 mL, 1 M), and reaction temperature (25° C), with less intensity band evident at λ_{max} =465 nm in 8 h; (b) dopamine 1 mL, 2 × 10^{-3} M) in MeOH, MoO_3 (2.0 × 10^{-4} M), 30% H_2O_2 (1 mL, 2× 10^{-3} M), pH 7 phosphate buffer (1 mL, 1 M), and reaction temperature (25° C) were used, and no discernible band was found at λ_{max} =465 nm.

Reactivity of $[\{Mo^{VI}O_2\}_2(L^3)(H_2O)_2]$ 3 with H_2O_2

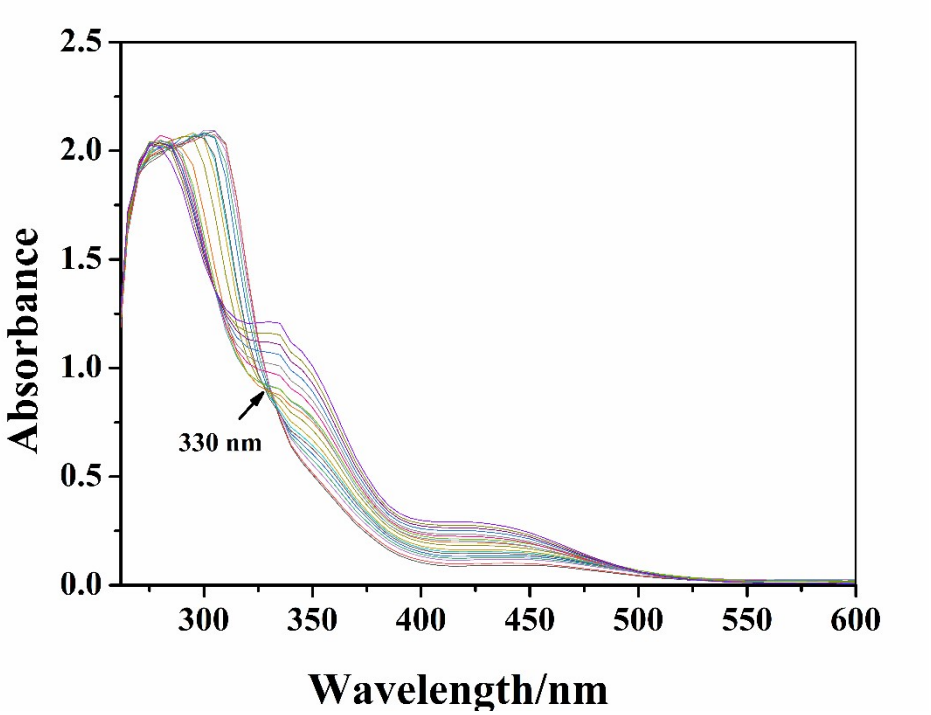

Fig. S25 UV-Visible spectrum marked changes during the titration of $[\{Mo^{VI}O_2\}_2(L^3)(H_2O)_2]$ **3** with H_2O_2. The spectra were obtained by gradually adding H_2O_2 (1 drop of 30% H_2O_2 in 5 mL DMSO) to 2.2×10^{-4} M solution of **3**.

During the catalytic reaction, in situ formation of oxidoperoxidommolybdenum(VI) intermediates can be observed and investigated using a UV-Visible spectrophotometer(Fig. S25). [1] Titration of 10 mL of DMSO solution of dioxido complex $[\{Mo^{VI}O_2\}_2(L^3)(H_2O)_2]$ **3** (**2.2** $\times 10^{-4}$ M) with 30 % H_2O_2 (one drop, 0.0072 g, 0.21 mmol) diluted in 5 mL of DMSO results in the shifting of a 280 nm band at 305 nm with a little change in intensity. After 7 drops of this diluted solution, there was no change in the intensity of band 305 nm. However, the intensity of bands at 335 nm and 425 nm shifted to the lower intensity, and an isosbestic point was noticed at 330 nm, indicating the generation of oxidoperoxidomolybdenum(VI) species that transfer their oxygen to the substrate, causing the production of oxidised substrate product. [1, 2]

References

1. M. R. Maurya, N. Chaudhary, F. Avecilla and I. Correia, Mimicking peroxidase activity by a polymer-supported oxidovanadium (IV) Schiff base complex derived from salicylaldehyde and 1, 3-diamino-2-hydroxypropane, *J. Inorg. Biochem.*, 2015, **147**, 181–192.

2. M. R. Maurya, R. Tomar, L. Rana and F. Avecilla, Trinuclear Dioxidomolybdenum (VI) Complexes of Tritopic Phloroglucinol-Based Ligands and Their Catalytic Applications for the Selective Epoxidation of Olefins, *Eur. J. Inorg. Chem.,* 2018, **25**, 2952–2964.